Journal of Volcanology and Geothermal Research 259 (2013) 308–316

Contents lists available at SciVerse ScienceDirect

Journal of Volcanology and Geothermal Research

journal homepage: www.elsevier.com/locate/jvolgeores

# Photogrammetric monitoring of lava dome growth during the 2009 eruption of Redoubt Volcano

Angela K. Diefenbach [a,*], Katharine F. Bull [b], Rick L. Wessels [c], Robert G. McGimsey [c]

[a] Cascades Volcano Observatory, U.S. Geological Survey, 1300 SE Cardinal Court, Suite 100, Building 10, Vancouver, WA 98683, USA
[b] Alaska Volcano Observatory/Alaska Division of Geological and Geophysical Surveys, 3354 College Road, Fairbanks, AK 99708, USA
[c] Alaska Volcano Observatory, U.S. Geological Survey, 4210 University Drive, Anchorage, AK 99508, USA

ARTICLE INFO

*Article history:*
Received 1 June 2011
Accepted 21 December 2011
Available online 29 December 2011

*Keywords:*
Oblique photogrammetry
Dome volume
Dome extrusion rate
Redoubt Volcano

ABSTRACT

The 2009 eruption of Redoubt Volcano, Alaska, began with a phreatic explosion on 15 March followed by a series of at least 19 explosive events and growth and destruction of at least two, and likely three, lava domes between 22 March and 4 April. On 4 April explosive activity gave way to continuous lava effusion within the summit crater. We present an analysis of post-4 April lava dome growth using an oblique photogrammetry approach that provides a safe, rapid, and accurate means of measuring dome growth. Photogrammetric analyses of oblique digital images acquired during helicopter observation flights and fixed-wing volcanic gas surveys produced a series of digital elevation models (DEMs) of the lava dome from 16 April to 23 September. The DEMs were used to calculate estimates of volume and time-averaged extrusion rates and to quantify morphological changes during dome growth. Effusion rates ranged from a maximum of 35 $m^3\ s^{-1}$ during the initial two weeks to a low of 2.2 $m^3\ s^{-1}$ in early summer 2009. The average effusion rate from April to July was 9.5 $m^3\ s^{-1}$. Early, rapid dome growth was characterized by extrusion of blocky lava that spread laterally within the summit crater. In mid-to-late April the volume of the dome had reached $36\times10^6$ $m^3$, roughly half of the total volume, and dome growth within the summit crater began to be limited by confining crater walls to the south, east, and west. Once the dome reached the steep, north-sloping gorge that breaches the crater, growth decreased to the south, but the dome continued to inflate and extend northward down the gorge. Effusion slowed during 16 April–1 May, but in early May the rate increased again. This rate increase was accompanied by a transition to exogenous dome growth. From mid-May to July the effusion rate consistently declined. The decrease is consistent with observations of reduced seismicity, gas emission, and thermal anomalies, as well as declining rates of geodetic deflation or inflation. These trends suggest dome growth ceased by July 2009. The volume of the dome at the end of the 2009 eruption was about $72\times10^6$ $m^3$, more than twice the estimated volume of the largest dome extruded during the 1989–1990 eruption. In total, the 2009 dome extends over 400 m down the glacial gorge on the north end of the crater, with a total length of 1 km, width of 500 m and an average thickness of 200 m.

Published by Elsevier B.V.

## 1. Introduction

Measurements of the volume and rate of growth of active lava flows and domes are key parameters of volcano monitoring (Stevens et al., 1999; Hunter et al., 2003; Baldi et al., 2005; Harris et al., 2005; Schilling et al., 2008; Wadge et al., 2008; Coppola et al., 2010; James et al., 2010). These values can be used in conjunction with many datasets (e.g. gas geochemistry, seismicity, geodetic deformation, thermal flux) to better constrain our understanding of eruption dynamics (Iverson et al., 2006; James et al., 2006; Gerlach et al., 2008; Luckett et al., 2008). During eruption response, dome volume and rate of growth are also critical factors to provide effective assessment of volcanic hazards, particularly during dome-building eruptions where changes in eruptive conditions can initiate dome collapse and threaten societal assets on the ground and in the air (Watts et al., 2002; Sparks et al., 1998; Nakada et al., 1999; Calder et al., 2002).

Hazards associated with dome collapse are especially relevant to Redoubt Volcano, Alaska (Fig. 1). During the 1989–1990 eruption of Redoubt Volcano, 14 lava domes were extruded, of which 13 collapsed by gravitational force and explosive activity, causing large ash clouds that wreaked havoc for air traffic and local communities in the Cook Inlet region (Casadevall, 1994; Miller, 1994). A problem during the 1989–1990 eruption response was the inability to assess dome size, volume and growth rates rapidly. Often, such measurements were difficult to attain due to hazardous conditions, limited daylight, lack of resources and/or time constraints.

After 19 years of eruptive repose and several months unrest (Bull and Buurman, 2013), an eruption began at Redoubt Volcano with a phreatic explosion on 15 March 2009. A series of 19 major explosions

* Corresponding author at: U.S. Geological Survey, Cascades Volcano Observatory, 1300 SE Cardinal Court, Bldg 10, Suite 100, Vancouver, WA 98683, USA. Tel.: +1 360 993 8957; fax: +1 360 993 8980.
*E-mail address:* adiefenbach@usgs.gov (A.K. Diefenbach).

0377-0273/$ – see front matter. Published by Elsevier B.V.
doi:10.1016/j.jvolgeores.2011.12.009

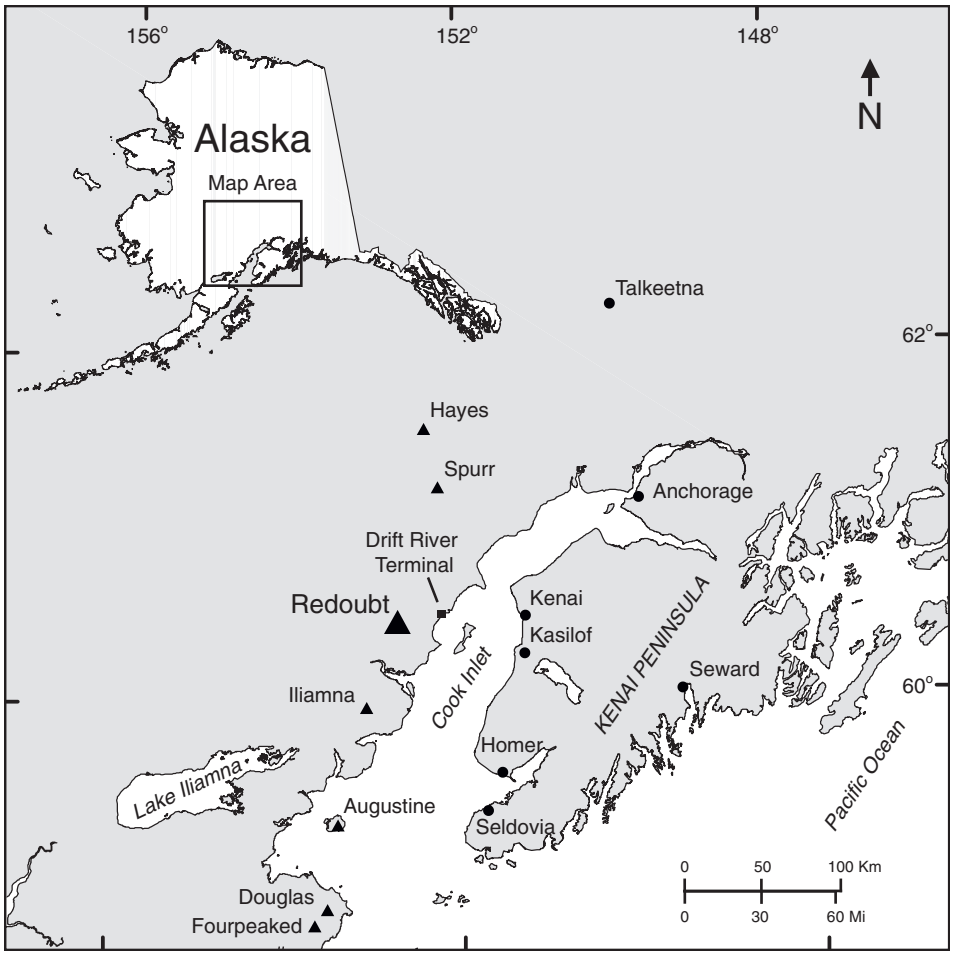


**Fig. 1.** Location map of Redoubt Volcano and other Cook Inlet volcanoes (black triangles) as well as nearby communities and locations mentioned in the text.

occurred between 22 March and 4 April, each sending ash clouds more than 5 km into the atmosphere. During this time, visual and seismic observations suggest that two and possibly three lava domes grew inside the 2009 explosion crater just south of the last dome emplaced in 1990. All three domes were subsequently destroyed by explosions. On 4 April the largest and final explosion occurred, resulting in the removal of previously emplaced 2009 material as well as most, if not all, of the remaining 1990 dome material. This explosion sent an ash cloud to 18 km above sea level (a.s.l.) that traveled southeast over nearby communities, produced pyroclastic flows and caused lahars in excess of $60\times10^6$ m$^3$ that extended 40 km down the Drift River Valley (Bull and Buurman, 2013; Schaefer, in press; Schneider and Hoblitt, 2013; Wallace et al., 2013; Waythomas et al., 2013). Following the 4 April event, the explosive phase of the eruption ended and was followed by a period of continuous extrusion that produced the fourth lava dome of the eruption.

Concern regarding the activity and stability of the lava dome during this effusive phase led to the application of a safe, rapid and effective photogrammetry approach to quantify dome growth. Like previous studies that have used photogrammetry to model and study active volcanic processes (Cecchi et al., 2003; Donnadieu et al., 2003; Herd et al., 2005; Schilling et al., 2008; Wadge et al., 2008; Darnell et al., 2010; Ryan et al., 2010; Wadge et al., 2010; Diefenbach et al., 2011), oblique photogrammetry was employed during the 2009 Redoubt Volcano eruption to produce a series of digital elevation models (DEMs) of the growing lava dome. We used the DEMs to calculate dome volumes and time-averaged extrusion rates, and to evaluate evolving dome morphology and assess potential hazards. We will show that oblique photogrammetry is a flexible and rapid tool for monitoring lava dome growth, especially when used in conjunction with other monitoring techniques. Here, we describe the growth of dome 4 during the last effusive phase of the eruption from April to July and compare and contrast the 1989–1990 and 2009 dome-building eruptions.

## 2. Methods

During the 2009 eruption of Redoubt Volcano, visual observation and FLIR (Forward Looking Infrared Radiometer) helicopter flights as well as fixed-wing airplane gas surveys provided platforms to acquire hand-held oblique imagery of the growing lava dome. These photographs were processed using a simple and accurate oblique photogrammetry method to produce a series of DEMs from which volume, subsequent time-averaged extrusion rates and morphological changes were quantified. Typically, imagery was processed and volume and rates calculated within a few hours of acquisition, which enabled rapid analysis of dome growth and evaluation of potential volcano hazards during the ongoing eruption response.

The photogrammetric software PhotoModeler Pro[1] was used for this study and provides a general case geometric solution for a series of convergent (typically 45°) oblique images where some exterior control and interior camera parameters, such as ground control and camera focal length, are known. Oblique images of the dome were acquired with a digital single lens reflex (SLR) camera (Nikon D70, Nikkor 24–120 mm lens, 6 megapixel resolution) and a lens set at a fixed focal length of 24 mm. Photographs were taken at various

[1] Use of trade names in this manuscript is for identification purposes only and does not constitute endorsement by the U.S. Geological Survey.

altitudes (250–1800 m) above and distances (1–4 km) from the dome, and provided almost 360 degree coverage of the dome when atmospheric and volcanic conditions (i.e. dense steam or ash plumes, low cloud-cover) permitted (Fig. 2a). The location of the aircraft at the time each photograph was captured was calculated by the photogrammetric software with the input of ground control coordinates through the process of resection. Ground control targets to constrain model geometry and spatial orientation could not be deployed during the eruption due to difficult access and hazardous conditions, so control points were obtained by choosing features recognizable in oblique images and on a 10 m DEM of Redoubt Volcano made from 1990 topographic data (Fig. 2b–c). A minimum of four ground control points (GCPs) were input into each model for exterior orientation and an additional six to ten homologous points were identified to spatially tie series of images together. Interior orientation was achieved through camera calibration by means of an automated calibration procedure with input of photographs of a gridded calibration target taken at different angles. Topographic reconstruction of the dome was completed with manual identification of common points in pairs and series of photographs. The average ground sample distance, represented in meters per pixel, in the area of the dome was 1 m. Each pair of sequential photographs (a photogrammetric model) yielded a cloud of three-dimensional points (average of 1,000 points) having irregular spacing.

Post-processing of the photogrammetric data was carried out using ArcGIS 9 software. Spatial coordinates from each photogrammetry model were triangulated by means of Delaunay triangulation to construct a series of triangulated irregular networks (TINs). TINs were interpolated to 10 m raster DEMs, a resolution consistent with the pre-eruption DEM used for volume calculations (Fig. 2b). Volumes were calculated by subtracting a pre-eruption (basal) surface model from each new successive dome DEM. Topographic reconstruction of a basal surface was estimated by projecting the lowest (z-value) of the dome base, identified in the first photogrammetry model (16 April), across the crater floor. This surface was merged with the part of the 1990 DEM that represented pre-eruption topography of the gorge at the breach of the north side of the crater to provide a more accurate account of basal topography where it was known. Each successive volume measurement includes newly extruded material retained on the lava dome. Rockfall events during the last effusive phase happened infrequently and those that did occur were small and probably did not remove significant amounts of dome material. No attempt was made to estimate the amount of material removed by these rockfall events. Time-averaged extrusion rates were calculated by dividing the net volume change by the elapsed time between successive photogrammetric surveys. A detailed technical description of the oblique photogrammetry approach is given by Diefenbach et al. (2011).

## 3. Dome growth

A series of 8 DEMs were constructed that documented dome growth of the final dome (dome 4) during the last effusive phase of the eruption between 16 April and 1 July 2009 (Table 1; Fig. 3). During this time, dome growth was continuous. An additional two post-eruption (20 August and 23 September) DEMs were constructed for monitoring purposes and to confirm the final dome volume (Table 1; Fig. 3). We used these data, combined with visual observations, to quantify the evolution of dome 4 and estimate the total erupted dome volume during the 2009 Redoubt Volcano eruption using an average magma discharge rate.

Following the 4 April explosive event, FLIR and satellite data suggest that the growth of dome 4 began within the excavated summit crater (Fig. 4a). Direct confirmation of lava dome growth came from

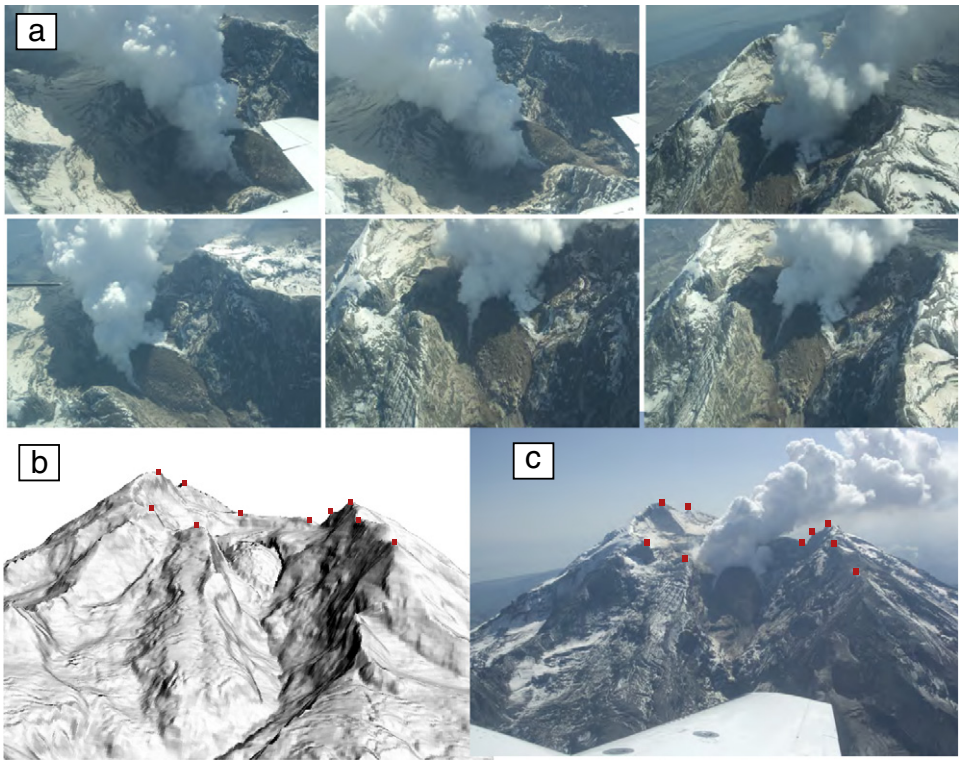


**Fig. 2.** a. An example of a series of oblique convergent images taken of the lava dome on 26 May 2009 during a fixed-wing gas survey. These images were later used to estimate dome volume using photogrammetric techniques described in the text. b. Shaded relief image of Redoubt Volcano showing edifice topography and 26 May 2009 lava dome. Topographic data from 1990 DEM; lava dome configuration from oblique photogrammetry techniques described in text. View is toward the south. c. Oblique image from 26 May having the same perspective as the shaded relief image. Red boxes in b and c represent control points used in photogrammetric analyses.

**Table 1**
Dome volume and effusion rate calculations syn- (April to July) and post-eruption (August to September) at Redoubt. Associated error estimates are rounded to one significant figure.

| Date (MM/DD/YYYY) | Observation platform | Volume ($10^6$ m$^3$) | Effusion rate (m$^3$ s$^{-1}$) |
|---|---|---|---|
| 04/04/2009 | Dome 4 effusion begins | | |
| | | | 35 ± 1.0 |
| 04/16/2009 | Helicopter | 36 ± 1.0 | |
| | | | 4.2 ± 0.8 |
| 05/04/2009 | Fixed-wing | 42 ± 0.6 | |
| | | | 14 ± 2.0 |
| 05/08/2009 | Helicopter | 47 ± 0.6 | |
| | | | 14 ± 4.0 |
| 05/14/2009 | Fixed-wing | 54 ± 1.8 | |
| | | | 27 ± 12 |
| 05/16/2009 | Helicopter | 59 ± 1.0 | |
| | | | 4.7 ± 1.0 |
| 05/26/2009 | Fixed-wing | 63 ± 0.6 | |
| | | | 3.8 ± 0.6 |
| 06/09/2009 | Helicopter | 68 ± 0.4 | |
| | | | 2.2 ± 0.4 |
| 07/01/2009 | Helicopter | 72 ± 0.6 | |
| 08/20/2009 | Helicopter | 71 ± 2.0 | – |
| 09/23/2009 | Helicopter | 70 ± 0.3 | – |

the first clear views during an observation flight on the 16 April. Initial dome growth was characterized by rapid extrusion of blocky lava that spread laterally from a single vent within the summit crater (Fig. 4b–c). On 16 April, twelve days of effusion had filled the summit crater with $36\times10^6$ m$^3$ of lava at an average rate of 35 m$^3$ s$^{-1}$ (Table 1; Fig. 3). By this time, dome growth was limited by the crater walls to the south, east and west and the toe of the dome had reached the breach on the north side of the crater (Fig. 4b–c). A talus apron had also developed on the north side of the dome that covered an area of roughly 43,000 m$^2$ (~15% of dome area) (Figs. 4b–c; 5). From the 16 April to the 4 May, effusion had slowed significantly to about 4.2 m$^3$ s$^{-1}$ (Fig. 3). Primary growth was focused near the toe of the lava dome, which had advanced more than 200 m (average advancement rate of ~11 m d$^{-1}$) down the gorge (Figs. 4e; 5; 6).

The effusion rate abruptly increased to 14 m$^3$ s$^{-1}$ between 4 May and 8 May and by 8 May the dome had a volume of $47\times10^6$ m$^3$ (Table 1; Fig. 3). Interestingly, this increase in extrusion rate in early May corresponds to a transition in dome morphology from a blocky lava (blocks 5–42 m in diameter) to a more rubbly (blocks <1 to 9 m in diameter), darker surface (Fig. 4b–h). The primary process of growth also transitioned from accelerated advancement of the flow front to inflation or accumulation of material from a central spreading center (Figs. 4g; 5; 6). From 5–6 May, a swarm of repeating earthquakes occurred and it contained the greatest number of events during the last effusive phase of the eruption (Buurman et al., 2013; Haney et al., 2013). The swarm also was associated with elevated gas emissions of $CO_2$ and $SO_2$ (Werner et al., 2013).

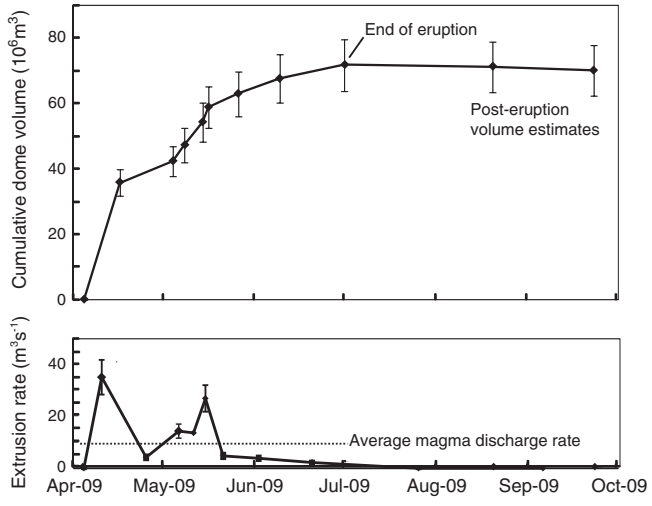


**Fig. 3.** Cumulative dome volume and time-averaged extrusion rates during the last effusive phase of the 2009 eruption. Additional dome volumes were calculated for dates in August and September 2009 for general monitoring purposes and to verify that dome growth had ceased and the eruption ended. Error bars represent the average uncertainty in volume change between successive dates (13%) and average effusion rates (20%).

Between 8 May and 14 May, extrusion rate remained relatively constant (14 m$^3$ s$^{-1}$) and the volume of the dome reached $54\times10^6$ m$^3$ (Table 1; Fig. 3). By 14 May, a significant portion of the northern talus apron had either been removed by continued rockfall activity, or was overridden by advancing dome lava. As of 14 May, the talus apron accounted for less than 5% of the dome area (Fig. 4f). The effusion rate doubled between 14 May and 16 May to 27 m$^3$ s$^{-1}$, adding an additional $4.6\times10^6$ m$^3$ of lava to the dome (Table 1; Fig. 3). From 16 May to the beginning of June, the rate of effusion declined and by 9 June the dome volume was about $68\times10^6$ m$^3$. From 9 June to 1 July, the rate of effusion was ~2.2 m$^3$ s$^{-1}$ (Table 1; Fig. 3).

Cessation of effusive activity occurred sometime after mid-June to early July. We use an end date of 1 July for the eruption, which is consistent with reduced levels of gas emission, seismicity and deformation (Fig. 4h). In addition, DEMs from August and September show a slight decrease in dome volume (note this is within the estimated error of each measurement), which may suggest relaxation of dome material, in the form of settling and slumping, in a post-eruption phase (Table 1; Fig. 3; Fig. 5). In total, the final dome extends over 400 m down the glacial gorge, with a total length of 1 km, maximum width of 500 m and average thickness of 200 m (Fig. 6). We estimate the total volume of andesitic lava erupted during the effusive phase to be $72\times10^6$ m$^3$ (Table 1; Fig. 3). Considering an emplacement time of 88 days, this equates to an average eruption rate of 9.5 m$^3$ s$^{-1}$ for the effusive phase of the eruption. To estimate the entire volume of dome material erupted during both the explosive and effusive phases, we extrapolate the magma supply rate of dome 4 to the time period of emplacement of the three previous domes. This yields a volume of $0.82\times10^6$ m$^3$ for dome 1 (assuming <1 day emplacement), $4.9\times10^6$ m$^3$ for dome 2 (assuming 6 day emplacement), $2.1\times10^6$ m$^3$ for dome 3 (assuming a 2.5 day emplacement) and a total erupted dome volume of $80\times10^6$ m$^3$ value for the entire 2009 eruption. This equates to a dense-rock equivalent (DRE) volume of $60\times10^6$ m$^3$ using a multiplicative correction factor of 0.75 (Bull et al., 2013; Coombs et al., 2013) that corrects the measured dome volume based on conservative vesicularity measurements of dome samples. Void space in talus was not incorporated in the correction factor because talus was not included in dome volume measurements. Vesicularity measurements of dome samples were highly variable and difficult to make because of the irregular vesicle shapes (see Bull et al., 2013), therefore there is considerable uncertainty in the measured values. High vesicularity measurements (> 40%; Bull et al., 2013) are likely representative of only a thin frothy carapace to a much more dense, less vesicular lava (e.g., Mount St. Helens 1980–1986; Cashman, 1988).

## 4. Data limitations and assumptions

Photogrammetric analyses incur both systematic and non-systematic error. Potential sources of error related directly to the design of the photogrammetric survey include camera calibration, sensor resolution, distance to object, ground control, precision of measurements in the imagery as well as random factors such as atmospheric conditions (i.e. steam, cloud cover), operator error and the nature and complexity of the terrain being modeled. Therefore assessment of error involved in terrain modeling is not always

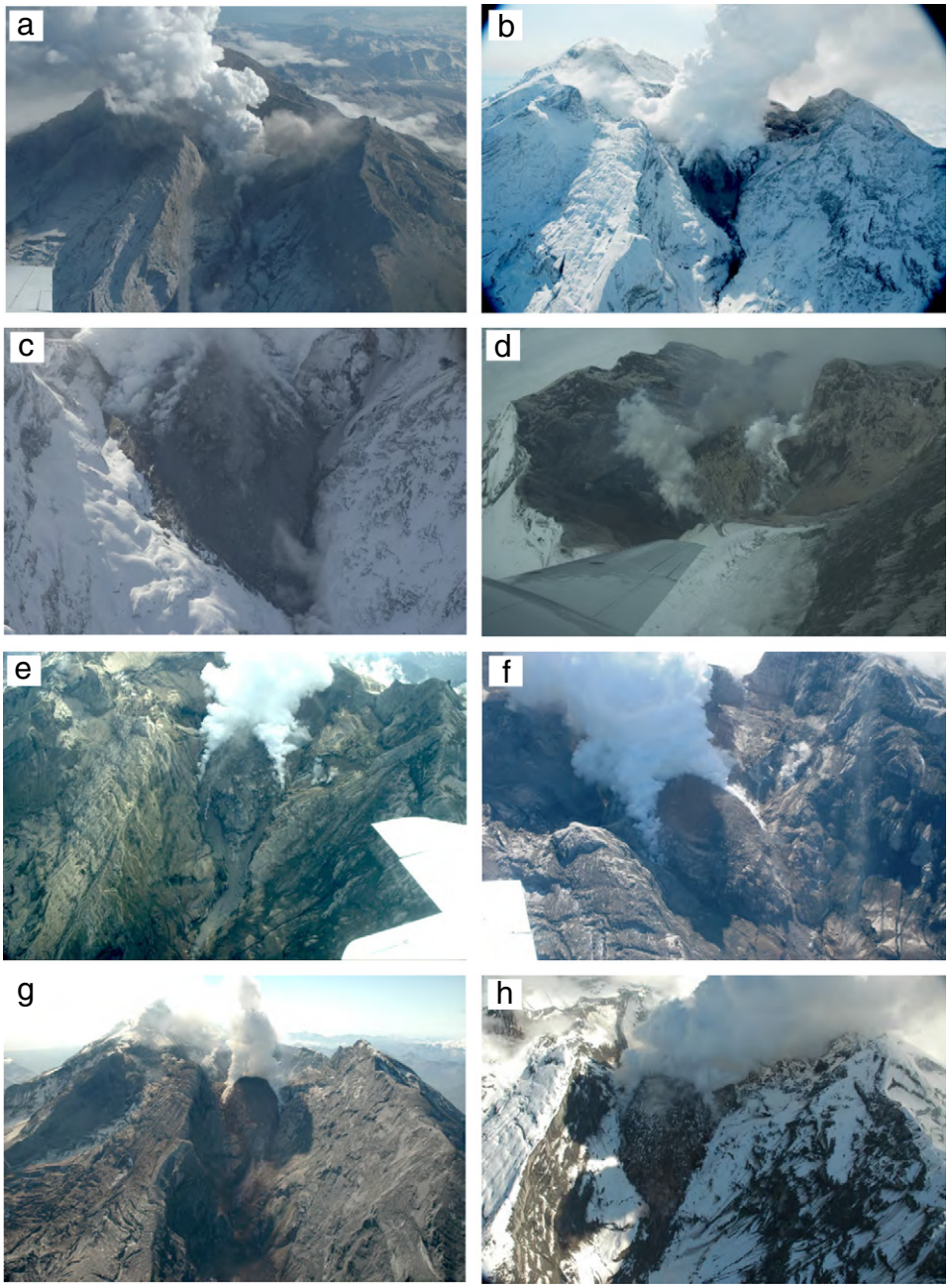


**Fig. 4.** a. Oblique photograph taken one day after final explosive event in 2009. Persistent steaming obscured direct observations of the lava dome that began growing within the excavated summit crater and it was not possible to obtain images useful for photogrammetric analysis of dome volume. b. 16 April 2009, nearly two weeks of dome growth filled the summit crater with a blocky lava dome. c. Close-up view, looking south, of the blocky lava dome on 16 April at the breach of the north side of the summit crater. An extensive talus apron surrounds the north side of the growing dome. d. First clear view of the south side of the lava dome on 28 April. e. Oblique images from 4 May showed the continued migration of dome growth north, down the steep glacial gorge and the initial transition of dome texture from blocky to rubbly. f. Exogenous dome growth continued on 16 May. By this date the talus apron was limited to 5% of the dome area. g. June 6 image captured radial block movement away from a slightly concave area on top of lava dome, which likely represented the surface expression of the vent. h. July 1 marked the end of the 2009 eruption. Minor snow accumulation was visible on the lava dome.

straightforward; particularly when using convergent, oblique imagery from a non-metric camera.

Using a calibrated camera reduced systematic errors. The accuracy of each photogrammetry model was determined from the root mean square (RMS) residual, which measures the difference between an operator-selected reference point and the expected coordinates calculated by the software. These coordinates are defined by the projection and ground control network. Any error associated with the ground control used to orient each model is propagated to the residuals of reference points. To calculate the uncertainty in volume estimates we propagated RMS residual values and uncertainty in GCP locations (i.e. 0.17 m; Schilling et al., 2008) throughout our calculations using standard error equations (e.g. Wolf and Ghilani, 1997) (Table 1). We estimate the average uncertainty in dome volume measurement to be $\pm 8.7\times10^5$ m$^3$ (1.5% of the average dome volume calculated from each DEM). Differencing measured elevation values increases the relative uncertainty of those measurements. We estimate the average uncertainty in volume change between successive DEMs to be $1.2\times10^6$ m$^3$ (about 13% of the average volume change). Error associated with extrusion rate values were calculated using standard error propagation methods (e.g. Stoer and Bulirsch, 2002) (Table 1). The uncertainty in time between photogrammetric surveys

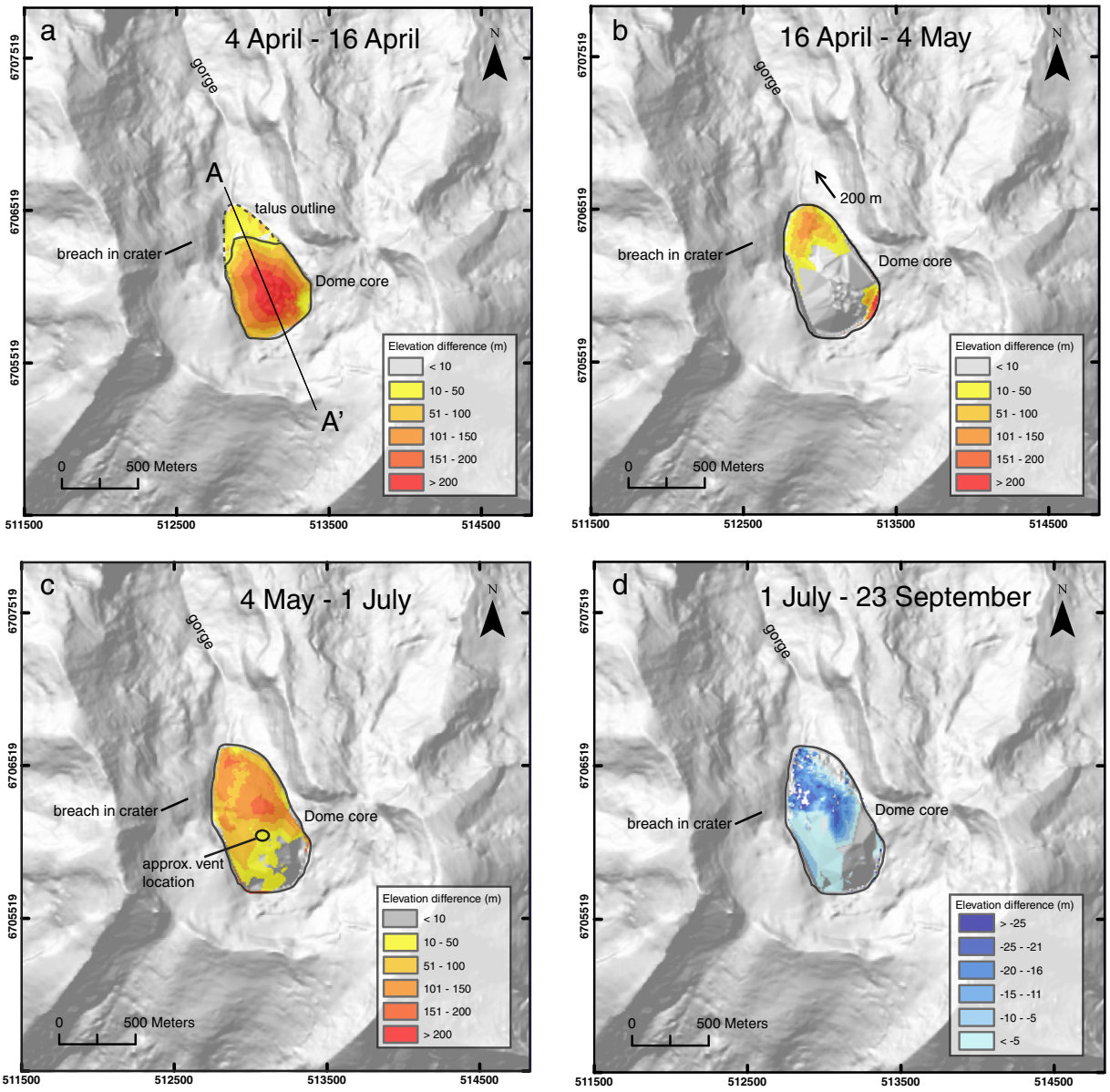


**Fig. 5.** Height difference maps that highlight changes in the locus of dome growth throughout the last effusive phase of the 2009 eruption. a. Dome height change from 4 April to 16 April—dome growth was focused within the summit crater. A to A′ line represents cross section in Fig. 6. b. 16 April to 4 May—dome growth was focused near toe of lava dome, which during this time had advanced more than 200 m north, down the gorge. c. 4 May to end of eruption 1 July—dome growth was focused from a central spreading center. Lava accumulation was predominately on the north side of the dome. d. Post-eruption dome changes from 1 July to 23 September. Central spreading center was the main focus of loss of dome height. Height loss may represent settling and slumping of dome material.

is the sum of the durations of the photo acquisition between successive dates. The average extrusion rate uncertainty is 2.8 $m^3 s^{-1}$; approximately 20% of the average of all extrusion rates.

Perhaps the largest source of uncertainty in the volume estimates comes from the assumed basal topography underlying the area of the new dome. As discussed in the methods section, to model the basal surface the lowest z-value found on the first photogrammetry model (16 April) was used to project a flat surface across the crater and was merged with the pre-eruption DEM of the gorge (Fig. 6). Visual observations of Redoubt Volcano shortly after the 4 April explosive event suggested explosive activity caused a deeply excavated crater. The flat base model of the summit crater is a conservative estimate of the volume and does not include subsurface volume of the explosion crater.

Photographic coverage of the southern portion of the dome was often hampered by persistent steaming from the contact of hot rock with snow, ice and ponded water. The first clear view of this section of the dome came twelve days after the first series of photographs were captured (16 April) (Fig. 4d). Subsequently, data that covered the south portion of the dome from nearly two weeks later were merged with the photogrammetry model of 16 April to provide a more comprehensive volume estimate. This assumption was based on visual observations that suggested dome growth had stagnated in the south by the 16 April, but nonetheless leads to uncertainty in the volume estimate reported for this date (Table 1, Fig. 3). In addition, the limited photographic coverage in the south led to a consistent underestimation of the southern extent of the dome. Comparison of DEMs with satellite imagery (i.e., Quickbird and WorldView) suggests the southern extent of each DEM is consistently underestimated, by as much as 50 m.

Furthermore, any short-term fluctuations in extrusion rate lasting hours to days could not be captured by these surveys which

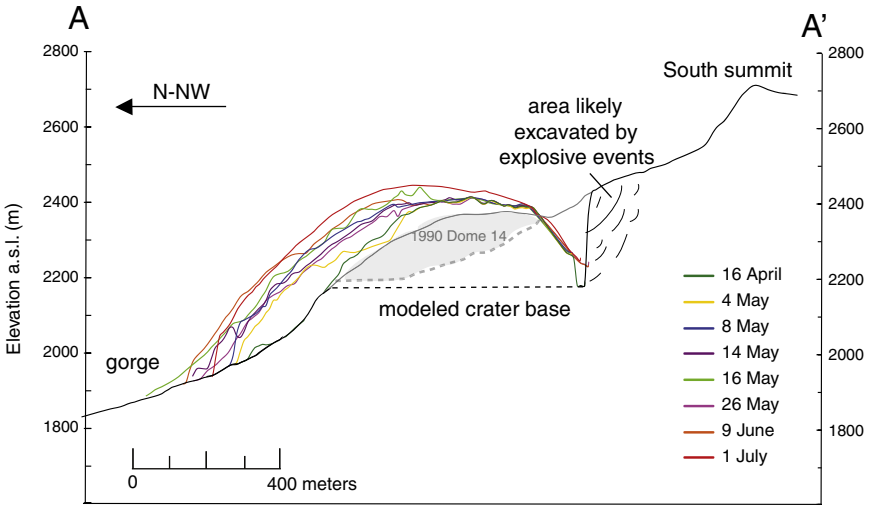


**Fig. 6.** Cross section of dome growth through time (16 April to 1 July 2009). Dashed line represents modeled basal surface used for volume calculations. The approximate surface extent of the final dome extruded in the 1989–1990 eruption of Redoubt is highlighted in gray. The unknown depth of the 1990 lava dome is represented by a dashed gray line.

were on average 11 days apart. Had access to the volcano been less restricted by weather and hazard conditions, an improved temporal resolution of observational flights and photogrammetric surveys may have helped us capture the short-term oscillatory nature of lava extrusion, particularly during the early stages of dome effusion.

## 5. Dome growth: 1989–1990 and 2009

The 2009 eruption of Redoubt Volcano has both similarities and differences to the previous eruption in 1989–1990. Both eruptions had periods of dome growth in the summit crater where lava extruded from a vent near the breach on the north side of the crater. Dome growth in 1989–1990 consisted primarily of episodic, short-lived, moderate-to-high-flux rate extrusion of blocky lava (Fig. 7a). Between 22 December 1989 and 15 June 1990, 14 domes were extruded and 13 subsequently destroyed, primarily by gravitational collapse (Miller, 1994). Most of the individual domes persisted for 3–9 days before being destroyed, the longest period of continuous effusion occurred over 55 days during the growth of the final dome (Miller, 1994) (Fig. 8). Throughout the 1989–1990 eruption, the rate of lava effusion progressively declined from about 26 to 2.1 $m^3\,s^{-1}$ and the average effusion rate for all episodes of dome growth was 5.8 $m^3\,s^{-1}$ (Miller, 1994). Total erupted dome volume during the 1989–1990 eruption is estimated at $88\times10^6\,m^3$ (Miller, 1994) (Fig. 8).

The 2009 magma supply rate was oscillatory, with pulses of high extrusion in between periods with lower rates. Bull et al. (2013) show that early dome growth was characterized by blocky lava that transitioned to a finer, rubbly texture (Fig. 7b). The longest period of continuous effusion lasted 88 days during the growth of dome 4 (Fig. 8). The range of effusion rates is similar to that for 1989–1990; 35 $m^3\,s^{-1}$ to 2.2 $m^3\,s^{-1}$, but the average lava discharge rate during the 2009 eruption (about 9.5 $m^3\,s^{-1}$) is nearly twice that of 1989–1990. In addition, the largest dome erupted in 2009 ($72\times10^6\,m^3$) is more than twice the estimated volume of the largest dome extruded in 1989–1990 ($30\times10^6\,m^3$; Miller, 1994) (Fig. 7c–d).

The variations between volumes reported for each eruption are influenced by the use of different surveying techniques. The 1989–1990 dome volumes were estimated assuming a conical shape based on dimensions from rough helicopter altimeter and electronic distance measurement (EDM) points of the summit and base, qualitative comparison of photographs and visual field estimates, when weather and hazard conditions permitted (Miller, 1994). In 2009, oblique photogrammetry permitted the three-dimensional reconstruction of the dome topography, providing a more accurate measure of dome volume, extrusion rate and error. Moreover, the oblique photogrammetry technique has been tested at other eruptions, most notably during the 2004–2008 eruption of Mount St. Helens where volume estimates were consistently within 5% of those made by traditional vertical photogrammetry (Diefenbach, 2007; Diefenbach et al., 2011). Fig. 7c–d illustrates the potential uncertainties in dome volume reporting between the two eruptions based on qualitative comparison of the largest domes from each eruption.

With the exception of the first three domes extruded in 2009, which were destroyed by explosive activity, the most remarkable difference between the two episodes of dome growth is the stability of the final dome extruded during the 2009 eruption. Bull et al. (2013) suggest the stability of the dome is likely a function of lava mechanics (mode of dome growth) as reflected by the transition in lava dome texture during the last effusive phase. The transition in style of growth in early May 2009, from endogenous blocky lava to exogenous scoriaceous lava, was concurrent with an increase in seismicity (Buurman et al., 2013; Haney et al., 2013) and $CO_2$ and $SO_2$ gas emissions (Werner et al., 2013). The high vesicularity of the scoriaceous lava may be evidence of efficient gas release from the conduit (Bull et al., 2013; Werner et al., 2013). Perhaps this gas exsolution slowed magma ascent rates enough to eventually cap the system before volumetric overpressure or over steepening of the flow-front could induce gravitational collapse of the dome.

We suggest that local topography, either independently or coupled with lava mechanics, may have played a role in the stability of the final dome extruded during the 2009 eruption. In 1989–1990 all 14 domes were tightly confined by ice and bedrock on three sides and were forced to grow vertically and eventually north down the steep gorge. Miller (1994) attributes the majority of the dome failures in 1989–1990 to the recurrent development of an over steepened flow front. The small crater where dome growth was focused left little room for dome growth to propagate to the south. Miller (1994) estimated that only 20% of the summit crater floor was occupied by any single dome during the 1989–1990 eruption. In contrast, the explosive activity at the onset of the 2009 eruption caused significant excavation of the summit crater, leaving a funnel-shaped crater several hundred meters across and as much as a few hundred meters

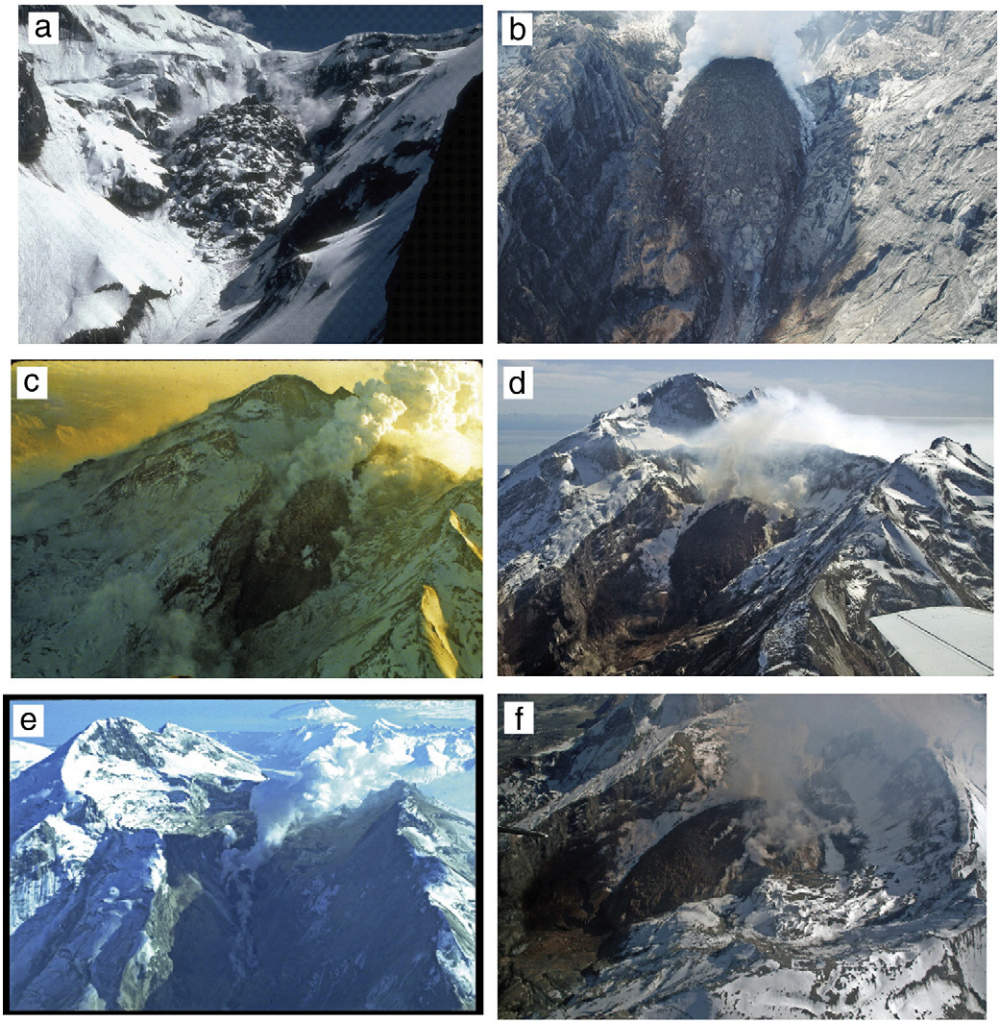


**Fig. 7.** a. June 1990 image of final lava dome extruded during 1989–1990 eruption. Illustrates typical blocky texture of lava domes extruded during the 1989–1990 eruption. b. June 2009 image of the lava dome from a similar vantage point. The surface of the lava dome was dominated by a more rubbly texture than that of 1990 dome. c. View to the south east of the largest dome extruded during the 1989–1990 eruption estimated at $30\times10^6\,m^3$ (Miller, 1994). The southern extent of the dome was restricted by summit ice. d. View to the south east of final 2009 lava dome estimated to be $72\times10^6\,m^3$, more than twice the largest 1989–1990 dome (c). The 2009 dome extends more than 400 m down the glacial gorge. e. View to the south of a typical small-volume lava dome erupted in the later stages of the 1989–1990 eruption. The dome was constrained to the north side of the summit crater. f. View to the east of the final 2009 lava dome which extends more than 200 m south in the summit crater than any dome during the 1989–1990 eruption.

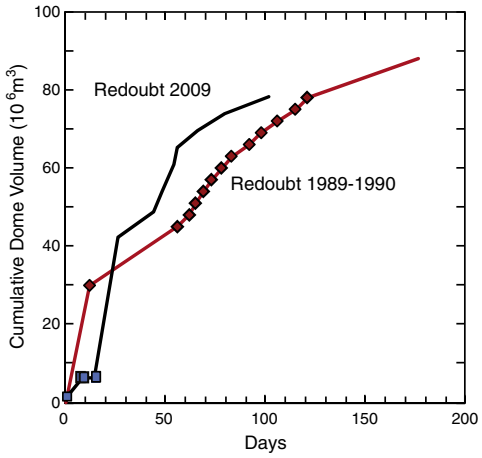


**Fig. 8.** Comparison of dome growth duration and cumulative volume during the 1989–1990 and 2009 eruptions of Redoubt. Each diamond and square marks the beginning of the growth of an individual lava dome in 1989–1990 and 2009, respectively.

deep. The large open crater allowed the dome lava to spread laterally before it encountered the steep topography in the upper Drift glacier gorge. Consequently, the final 2009 dome extends over 200 m beyond the southern extent of the final 1989–1990 dome and covers more than 75% of the summit crater. As in 1989–1990, growth of the final 2009 lava dome also began to flow preferentially to the north and down the gorge, but the 2009 summit crater provided storage room for a significant portion of the dome, which was therefore not subject to gravitational instability.

Further investigations of the dome structure and subsurface are required to fully understand the mechanisms responsible for the stability of dome growth during the effusive phase of the 2009 eruption. The dynamic nature of eruptions and volcanic systems suggest several processes may have contributed to the stability of dome 4. Although the fourth lava dome of the 2009 eruption remained intact throughout the effusive phase, its presence creates a significant hazard in the event of reactivation of Redoubt Volcano's magmatic system. Independent of what factors may be responsible for the stability of the final 2009 lava dome any new pulse of magma will likely follow the existing conduit and lava extrusion could cause structural instability of the 2009 dome that could culminate in partial or wholesale dome-collapse.

## 6. Summary

Oblique photogrammetry surveys during the last effusive phase of the 2009 eruption of Redoubt Volcano enabled measurement of dome volume and extrusion rate as well as supplemented visual observations to evaluate evolving dome morphology and hazards. This approach to monitoring dome growth allowed us to make estimates of dome volume and effusion rate where other types of ground based measurements would have been impractical. The photogrammetric analysis contributed to a detailed dome growth chronology and understanding of the lava dome and eruption processes operating during the eruption, and provided a convincing demonstration of the utility of digital photographs collected during routine observation flights in tracking and understanding an ongoing dome-building eruption.

## Acknowledgements

We thank the entire staff of the Alaska Volcano Observatory and members of the eruption response team for assistance in acquiring oblique photography used in this study. We thank Richard Herd, Steve Schilling, and Geoff Wadge for their reviews, which improved the clarity of this manuscript.

## References

Baldi, P., Fabris, M., Marsella, M., Monticelli, R., 2005. Monitoring the morphological evolution of the Sciara del Fuoco during the 2002–2003 Stromboli eruption using multi temporal photogrammetry. ISPRS Journal of Photogrammetry and Remote Sensing 59, 199–211.

Bull, K.F., Buurman, H., 2013. Eruption of Redoubt Volcano: an overview. Journal of Volcanology and Geothermal Research 259, 2–15.

Bull, K.F., Anderson, S.W., Diefenbach, A.K., Wessels, R.L., Henton, S.M., 2013. Emplacement of the final lava dome of the 2009 eruption of Redoubt Volcano, Alaska. Journal of Volcanology and Geothermal Research 259, 334–348.

Buurman, H., West, M.E., Thompson, G., 2013. The seismicity of the 2009 Redoubt eruption. Journal of Volcanology and Geothermal Research 259, 16–30.

Calder, E.S., Luckett, R., Sparks, R.S.J., Voight, B., 2002. Mechanisms of lava dome instability and generation of rockfalls and pyroclastic flows at Soufrière Hills Volcano, Montserrat. In: Druitt, T.H., Kokelaar, B.P. (Eds.), The Eruption of Soufrière Hills Volcano, Montserrat from 1995 to 1999: Geological Society of London Memoir, 21, pp. 173–190.

Casadevall, T.J., 1994. The 1989–1990 eruption of Redoubt Volcano, Alaska: implications on aircraft operations. Journal of Volcanology and Geothermal Research 62, 519–530.

Cashman, K.V., 1988. Crystallization of Mount St. Helens 1980–1986 dacite: a quantitative textural approach. Bulletin of Volcanology 50, 194–209.

Cecchi, E., van Wyk de Vries, B., Lavest, J.M., Harris, A., Davies, M., 2003. N-view reconstruction: a new method for morphological modeling and deformation measurement in volcanology. Journal of Volcanology and Geothermal Research 123, 181–201.

Coombs, M.L., Sisson, T.W., Bleick, H.A., Henton, S.M., Nye, C.J., Payne, A.L., Cameron, C.E., Larsen, J.F., Wallace, K.L., Bull, K.F., 2013. Andesites of the 2009 eruption of Redoubt Volcano, Alaska. Journal of Volcanology and Geothermal Research 259, 349–372.

Coppola, D., James, M.R., Staudacher, T., Cigolini, C., 2010. A comparison of field- and satellite-derived thermal flux at Piton de la Fournaise: implications for the calculation of lava discharge rate. Bulletin of Volcanology 72, 341–356.

Darnell, A.R., Lovett, A.A., Barclay, J., Herd, R.A., 2010. An application-driven approach to terrain model construction. International Journal of Geographic Information Science 37, 1171–1191.

Diefenbach, A.K., 2007. Oblique photogrammetric analysis of the dome-building eruption of Mount St. Helens, 2004–2007: MS thesis, Western Washington University, 103 pp.

Diefenbach, A.K., Crider, J.G., Schilling, S.P., Dzurisin, D., 2011. Rapid, low-cost photogrammetry to monitor volcanic eruptions: an example from Mount St. Helens, Washington, USA. Bulletin of Volcanology. doi:10.1007/s00445-011-0548-y.

Donnadieu, F., Kelfoun, K., van Wyk de Vries, B., Cecchi, E., Merle, O., 2003. Digital photogrammetry as a tool in analogue modeling: applications to volcano instability. Journal of Volcanology and Geothermal Research 123, 161–180.

Gerlach, T.M., McGee, K.A., Doukas, M.P., 2008. Emission rates of CO2, SO2, H2S, scrubbing, and preeruption excess volatiles at Mount St. Helens, 2004–2005. In: Sherrod, D.R., Scott, W.E., Stauffer, P.H. (Eds.), A volcano rekindled: the renewed eruption of Mount St. Helens, 2004–2006: US Geological Survey Professional Paper, vol. 1750, pp. 543–571.

Harris, A., Dehn, J., Patrick, M., Calvari, S., Ripepe, M., Lodato, L., 2005. Lava effusion rates from hand-held thermal infrared imagery: an example from the June 2003 effusive activity at Stromboli. Bulletin of Volcanology 68, 107–117.

Haney, M.M., Chouet, B.A., Dawson, P.B., Power, J.A., 2013. Character of the long-period and very-long-period seismic wave field during the 2009 eruption of Redoubt Volcano, Alaska. Journal of Volcanology and Geothermal Research 259, 77–88.

Herd, R.A., Edmonds, M., Bass, V.A., 2005. Catastrophic lava dome failure at Soufriere Hills Volcano, Montserrat, 12–13 July 2003. Journal of Volcanology and Geothermal Research 148, 234–252.

Hunter, G., Pinkerton, H., Airey, R., Calvari, S., 2003. The application of long-range laser scanning for monitoring volcanic activity on Mount Etna. Journal of Volcanology and Geothermal Research 123, 203–210.

Iverson, R.M., Dzurisin, D., Gardner, C.A., Gerlach, T.M., LaHusen, R.G., Lisowski, M., Major, J.J., Malone, S.D., Messerich, J.A., Moran, S.C., Pallister, J.S., Qamar, A.I., Schilling, S.P., Vallance, J.W., 2006. Dynamics of seismogenic volcanic extrusion at Mount St. Helens in 2004–2005. Nature 444, 439–443.

James, M.R., Robson, S., Pinkerton, H., Ball, M., 2006. Oblique photogrammetry with visible and thermal images of active lava flows. Bulletin of Volcanology 69, 105–108.

James, M.R., Pinkerton, H., Ripepe, M., 2010. Imaging short period variations in lava flux. Bulletin of Volcanology 72, 671–676.

Luckett, R., Loughlin, S., De Angelis, S., Ryan, G., 2008. Volcanic seismicity at Montserrat, a comparison between the 2005 dome growth episode and earlier dome growth. Journal of Volcanology and Geothermal Research 177, 894–902.

Miller, T.P., 1994. Dome growth and destruction during the 1989–1990 eruption of Redoubt Volcano. Journal of Volcanology and Geothermal Research 62, 197–212.

Nakada, S., Shimizu, H., Ohta, K., 1999. Overview of the 1990–1995 eruption of Unzen Volcano. Journal of Volcanology and Geothermal Research 89, 1–22.

Ryan, G.A., Loughlin, S.C., James, M.R., Jones, L.D., Calder, E.S., Christopher, T., Strutt, M.H., Wadge, G., 2010. Growth of the lava dome and extrusion rates at Soufrière Hills Volcano, Montserrat, West Indies: 2005–2008. Geophysical Research Letters 37, L00E08. doi:10.1029/2009GL041477.

Schaefer, J.R.G. (editor), in press. The 2009 eruption of Redoubt Volcano, Alaska: Alaska Division of Geological & Geophysical Surveys Report of Investigations 2011-5, xx p.

Schilling, S.P., Thompson, R.A., Messerich, J.A., Iwatsubo, E.Y., 2008. Use of digital aerophotogrammetry to determine rates of lava dome growth, Mount St. Helens, 2004 2005. US Geological Survey Professional Paper, 1750, pp. 145–167.

Schneider, D.J., Hoblitt, R.P., 2013. Doppler weather radar observations of the 2009 eruption of Redoubt Volcano, Alaska. Journal of Volcanology and Geothermal Research 259, 133–144.

Sparks, R.S.J., Young, S.R., Barclay, J., Calder, E.S., Cole, P., Darroux, B., Davies, M.A., Druitt, T.H., Harford, C., Herd, R., James, M., Lejeune, A.M., Loughlin, S., Norton, G., Skerrit, G., Stasiuk, M.V., Stevens, N.S., Toothill, J., Wadge, G., Watts, R., 1998. Magma production and growth of the lava dome of the Soufriere Hills Volcano, Monteserrat, West Indies: November 1995 to December 1997. Geophysical Research Letters 25, 3421–3424.

Stevens, N.F., Wadge, G., Murray, J.B., 1999. Lava flow volume and morphology from digitised contour maps: a case study at Mount Etna, Sicily. Geomorphology 28, 251–261.

Stoer, J., Bulirsch, R., 2002. Introduction to Numerical Analysis. Springer, Berlin. p. 9–36.

Wadge, G., Macfarlane, D.G., Odbert, H.M., James, M.R., Hole, J.K., Ryan, G., Bass, V., De Angelis, S., Pinkerton, H., Robertson, D.A., Loughlin, S.C., 2008. Lava dome growth and mass wasting measured by a time series of ground-based radar and seismicity observations. Journal of Geophysical Research 113, B08210. doi:10.1029/2007JB005466.

Wadge, G., Herd, R.A., Ryan, G., Calder, E.S., Komorowski, J.C., 2010. Lava production at Soufriere Hills Volcano, Montserrat: 1995–2009. Geophysical Research Letters 37, L00E03. doi:10.1029/2009GL041466.

Wallace, K.L., Shaefer, J.R., Coombs, M.L., 2013. Character,mass, distribution, and origin of tephra-fall deposits from the 2009 eruption of Redoubt Volcano, Alaska—Highlighting the significance of particle aggregation. Journal of Volcanology and Geothermal Research 259, 145–169.

Watts, R.B., Sparks, R.S.J., Young, S.R., 2002. Growth patterns and emplacement of the andesitic lava dome at Soufrière Hills Volcano, Montserrat. Geological Society of London Memoirs 21, 115–152.

Waythomas, C.F., Pierson, T.C., Major, J.J., Scott, W.E., 2013. Lahars and flowage hazards in the Drift River valley associated with the 2009 eruption of Redoubt Volcano. Journal of Volcanology and Geothermal Research 259, 389–413.

Werner, C., Kelly, P.J., Doukas, M., Lopez, T., Pfeffer, M., McGimsey, R., Neal, C., 2013. Degassing of $CO_2$, $SO_2$, and $H_2S$ associated with the 2009 eruption of Redoubt Volcano, Alaska. Journal of Volcanology and Geothermal Research 259, 270–284.

Wolf, P.R., Ghilani, C.D., 1997. Adjustment Computations: Statistics and Least Squares in Surveying and GIS. John Wiley and Sons, New York, USA. 564 pp.